01 Dec 2012

ZHENG Classification In Traditional Chinese Medicine Based On Modified Specular-free Tongue Images

Ratchadaporn Kanawong

Tayo Obafemi-Ajayi
Missouri University of Science and Technology, towd2@mst.edu

Jun Yu

Dong Xu

et. al. For a complete list of authors, see https://scholarsmine.mst.edu/ele_comeng_facwork/4833

Recommended Citation

R. Kanawong et al., "ZHENG Classification In Traditional Chinese Medicine Based On Modified Specular-free Tongue Images," *Proceedings - 2012 IEEE International Conference on Bioinformatics and Biomedicine Workshops, BIBMW 2012*, pp. 288 - 294, article no. 6470318, Institute of Electrical and Electronics Engineers, Dec 2012.
The definitive version is available at https://doi.org/10.1109/BIBMW.2012.6470318

ZHENG Classification in Traditional Chinese Medicine based on Modified Specular-free Tongue Images

Ratchadaporn Kanawong*, Tayo Obafemi-Ajayi*, Jun Yu * †, Dong Xu*, Shao Li‡ and Ye Duan*
**Computer Science Department and Informatics Institute, University of Missouri, Columbia, MO, USA*
†College of Automation Engineering, Qingdao University, China
‡MOE Key Laboratory of Bioinformatics and Bioinformatics Division,
TNLIST and Department of Automation, Tsinghua University, Beijing, China

Abstract—**Traditional Chinese Medicine practitioners usually observe the color and coating of a patient's tongue to determine ZHENG (such as Cold or Hot ZHENG) and to diagnose different stomach disorders including gastritis. In our previous work, we explored new modalities for clinical characterization of ZHENG in gastritis patients via tongue image analysis using various supervised machine-learning algorithms. We proposed a system that learns from the clinical practitioner's subjective data how to classify a patients health status by extracting meaningful features from tongue images based on color-space models. In this paper, we propose an enhancement to the ZHENG classification system: a coating separation technique using the MSF images such that feature extraction is applied only to the coated region on the tongue surface. The results obtained over a set of 263 gastritis patients (most of whom are either Cold Zheng or Hot ZHENG), and a control group of 48 healthy volunteers demonstrate an improved performance for most of the classification types considered.**

Keywords-**ZHENG classification; color space features; machine learning; Reflection components separation; Specular reflection; Chromaticity.**

I. Introduction

There has been a surge of research interest [1], [2], [3], [4], [5], [6], [7], [8] in the last decade in the imaging community on Traditional Chinese Medicine (TCM) applications. Inspection of the tongue is a key component in Chinese Medicine. For thousands of years, Chinese medical practitioners have diagnosed the health status of a patient's internal organs by inspecting the tongue, especially patterns on the tongue's surface [9]. The changes of tongue can objectively manifest the states of a disease, which can help differentiate syndromes, establish treatment methods, prescribe herbs and determine prognosis of disease. Hence, Chinese medical practitioners rely on computer-aided tongue image analysis to assist them make more accurate, consistent clinical diagnosis.

ZHENG (TCM syndrome), an integral part of Chinese Medicine theory [10], is defined as the TCM theoretical abstraction of the symptom profiles of individual patients. It is used as a guideline in TCM disease classification. ZHENG classification is a traditional diagnostic method to categorize the patients based on their different conditions. Tongue appearance and features has been a valuable diagnostic tool for TCM practitioners to determining ZHENG in patients.

In our previous work [9], we explored new modalities for clinical characterization of ZHENG in gastritis patients via tongue image analysis using various supervised machine-learning algorithms. Given that TCM practitioners usually observe the tongue color and coating to determine ZHENG (such as Cold or Hot ZHENG) and to diagnose different stomach disorders including gastritis. We proposed a system that learns from the clinical practitioner's subjective data how to classify a patients health status by extracting meaningful features from tongue images based on color-space models. Thus, using machine-learning techniques, we establish the relationship between the color features extracted from the tongue images and ZHENG by learning through examples. The experimental results obtained demonstrate a great performance of the system. Our goal in this work is to enhance the performance and accuracy of the system.

The two main features of the tongue in TCM ZHENG differentiation and diagnosis are its color and coating. In this work, we propose a preprocessing step of separation of the coating on the tongue before feature extraction to enhance the accuracy of the ZHENG classification system. This is done using generating the Modified Specular-Free (MSF) [11] images of the tongue, as illustrated in Figure 1. Thus, we propose a coating separation technique using the MSF images such that feature extraction is applied only to the coated region on the tongue surface.

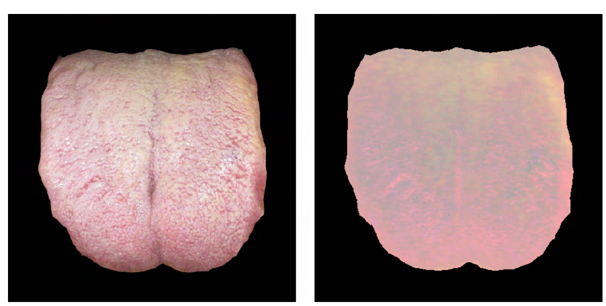

Figure 1. Illustration of an original tongue image and its MSF Image.

The proposed framework is as follows, given a tongue image of a patient, we apply the tongue segmentation method described in [8] to obtain the tongue only image. Next, we obtain the MSF image of the tongue using Shen et al. method [11] and extract the coated region of the tongue from it. Lastly, we apply color feature extraction to compute features for training and building our ZHENG classifier.

This paper is organized as follows: in Section II, we describe the proposed coating separation method using MSF Image while we present an overview of the feature set and classification models in Section III. The experimental results obtained are shown and analyzed in Section IV. Finally, the conclusion and future work is presented in Section V.

II. Coating Separation using MSF Image Technique

Our goal is to segment the coated region from tongue image so that we can apply feature extraction directly on this region as opposed to the entire tongue, like in our previous work [9]. As observed in Figure 2a, our method is based on the premise that the color of the coated region on the tongue is distinct from the remainder of the tongue. The color of the coated region can be yellow, white or even blue while the tongue body is usually of a reddish color.

In Figure 2, the RGB component of the tongue on the position of white line in Figure 2a is shown in Figure 2b. The color at the left and right boundary of the tongue is the actual color of tongue body. As can be observed, the red component is much higher than the other two components while for the middle part, which lies in the coated region, the values of the three components (red, blue and green) are not so distinct from each other. This property is similar to reflection. According to the dichromatic reflection model, the reflection of an arbitrary material derives from the linear combination between the diffuse reflection and specular reflection. Thus, our goal is to find both the diffuse reflection component and specular reflection components of the tongue image and use this information to separate the coated region from the non-coated region on the tongue.

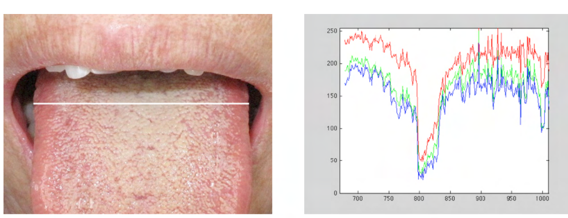

(a) (b)

Figure 2. The RGB component along the white line across tongue image (a) is illustrated in (b).

Tan et al. [12] introduced the concept of specular-free (SF) image, which maintains the geometrical information of the diffuse component. The purpose of SF image is to eliminate specular reflection component. Through the intensity logarithmic differentiation on both of the original and SF images, the pixels containing only diffuse reflections can be successfully localized. Shen et al. further improved on this via the modified specular-free [11] image to separate the diffuse and specular reflection components by the direct use of dichromatic reflection model. The SF image is obtained by subtracting the minimum RGB value at each pixel position, and the MSF image is formed by adding a same scalar value for each pixel on the SF image. The noise analysis indicates that the MSF image is more robust than the SF image, and therefore it is used to compute the chromaticity for each pixel. The approximate diffuse and specular candidates are decided according to the difference between the MSF and original images. Then, by iterative selection of body colors and calculation of chromaticity differences, the diffuse and specular reflection components are appropriately separated by the least- squares technique.

Let $I(p)$ is color intensity of the pixel p, denoted by $(R(p), G(p), B(p))$ which present in red, green, blue components respectively. I_{SF} and I_{MSF} stand for intensity of specular-free and modified specular-free respectively.

$$I_{SF}(p) = I(p) - I_{min}(p) \tag{1}$$

, where $I_{min}(p) = min(R(p), G(p), B(p))$

Let N denote the number of pixels belonging to region of interest (ROI).

$$I_{MSF}(p) = I_{SF}(p) + \frac{\sum_{p \in ROI} I_{min}(p)}{N} \tag{2}$$

The MSF image obtained is segmented into coated region and non-coated region using a given threshold. To determine the optimal threshold value for segmentation, we apply the Otsu's method [13] to each channel (red, green and blue) of the MSF image.

The goal of the Otsu algorithm is to compute an optimal threshold k^* for segmenting a grayscale image into a binary image of two classes C_0 and C_1. The image is represented by a normalized gray-level histogram of the intensity of all its pixels ranging from 1 to L gray levels. Thus a threshold value of k splits all the pixels of the image into two classes: $C_0 = \{1, 1, \ldots, k\}$ and $C_1 = \{k+1, k+2, \ldots, L\}$. Let p_i denote the probability of occurrence of a pixel in the image with intensity value i. The probabilities of the class occurrence can be expressed as:

$$\omega_0 = \sum_{i=1}^{k} p_i \quad \text{and} \quad \omega_1 = \sum_{i=k+1}^{L} p_i \tag{3}$$

The probabilities of the class mean levels can also be computed as:

$$\mu_0 = \sum_{i=1}^{k} ip_i/\omega_0 \quad \text{and} \quad \mu_1 = \sum_{i=k+1}^{L} ip_i/\omega_1 \tag{4}$$

The between-class variance σ_B^2 is defined as:

$$\sigma_B^2 = \omega_0\omega_1(\mu_1 - \mu_0)^2 \tag{5}$$

The optimal threshold k^* is the one that maximizes the between-class variance i.e.

$$\sigma_B^2(k^*) = \max_{1\leq k<L} \sigma_B^2(k) \tag{6}$$

Therefore, we select the optimal threshold value by apply applying the Otsu's method. When we observed the final segmentation derived from each channel, the red channel yielded the best representation of the coated region separated from the remainder of the tongue body. This is intuitive, given that the non-coated region on the tongue is mainly reddish in color. The coating separation process using the MSF image is illustrated in Figure 3. Figure 3d shows the MSF image segmented into the coated and non-coated region as represented by the green and red pixels respectively.

III. Feature Extraction and Classification Methods

A. Color Feature Set

Our goal is to compute a set of objective features $\vec{F_j} = \{F_n\}$ from the coated region of each tongue image j that can be fed into our learning system so that we can predict the color of the coating on the tongue as well as the different ZHENGs of the gastritis patients in relation to western medicine diagnosis. These features are designed to capture different color characteristics of the tongue using the color space model [2]. While a single feature may not be very discriminative, our premise is that the aggregation of these features will be discriminative. We leave it to the learning algorithm to determine the weight/contribution of each feature in the final classification.

We used a set of 25 features, developed in our previous work [9], that span the entire color space model. They are be grouped under eight categories: RGB, HSV, YIQ, Y'CbCr, XYZ, L*a*b*, L*u*v*, and CMYK. Table I gives a brief description of each category and the features computed from them. Ref [9] provides a full description of each category. All the features are normalized to a value between 0 and 1. Each feature f_i is computed per ith pixel in the coated region and then aggregated to obtain $\vec{F_j} = F_n$ per coated region of each tongue image j.

We model the ZHENG diagnosis differentiation task for gastritis patients as a classification problem. To train a classifier to learn from the clinical practitioner's labeled data, we need to combine the features per pixel into one composite feature vector $\vec{F_j} = F_n$ per tongue image (or region) j. We aggregate the pixel features using two different statistical averages (mean and median) and the standard deviation values. We derive six variations of feature vectors for the tongue ZHENG classification system using the following operators: mean ($\mu\vec{F}$), median ($med\vec{F}$), standard deviation ($\sigma\vec{F}$), "mean plus standard deviation" ($\{\mu\vec{F}, \sigma\vec{F}\}$), "median plus standard deviation" ($\{med\vec{F}, \sigma\vec{F}\}$), and "mean plus median plus standard deviation" ($\{\mu\vec{F}, med\vec{F}, \sigma\vec{F}\}$).

Given that N denotes the number of pixels in the coated region of a given tongue image j. The mean feature vector is denoted by $\mu\vec{F_j} = \{\mu F_n\}$, where μF_n is given by,

$$\mu F_n = \frac{\sum_{i=1}^{N} f_n^i}{N},\ n = 1, ..., 25. \tag{7}$$

The median feature vector, denoted by $med\vec{F_j} = \{medF_n\}$, is computed as $medF_n = midsort(F_{set})$, where n is the index of feature in a feature vector, therefore n can range from 1 to 25 in this case. $medF_n = mid\{sort(F_{set})\}$, $n = 1, \ldots, 25$. Standard deviation depicts the margin of difference between a given feature value and its average value among all the pixels in the given region. Thus, the standard deviation feature vector is denoted by $\sigma(\vec{F_j}) = \{\sigma F_n\}$, where σF_n is given by,

$$\sigma F_n = \sqrt{\frac{\sum_{i=1}^{N}(f_n^i - \mu F_n)}{N}},\ n = 1, ..., 25. \tag{8}$$

The "mean plus standard deviation" denoted by $\{\mu\vec{F}, \sigma\vec{F}\}$, is a concatenation of the mean feature vector and the standard deviation feature vector. Similarly, the "median plus standard deviation" feature vector, denoted by $\{med\vec{F}, \sigma\vec{F}\}$, is a concatenation of the median feature vector and the standard deviation feature vector. Thus, the total number of features in both concatenated feature vectors is 50 each.

The last feature vector "mean plus median plus standard deviation", denoted by $\{\mu\vec{F}, med\vec{F}, \sigma\vec{F}\}$ is a concatenation of all three: mean, median and the standard deviation feature vectors. It contains a total of 75 features.

B. Classification Methods

We apply three different supervised learning algorithms (Support vector machine (SVM), Multilayer perceptron network (MLP), Random Forest(RF)) to build classification models for training and evaluating the proposed ZHENG diagnosis system. In our previous work [9], we evaluated the Adaboost [18] as well as both the SVM and MLP classification models. The SVM and MLP outperformed the Adaboost for most of the experiments. However, a strength of the Adaboost is that it is a very simple ensemble classifier with very minimal number of parameters to optimize unlike the SVM and MLP. In this current work, we replace the Adaboost with the Random Forest [19], another simple ensemble classifier with minimal number of parameters to vary. Each model is described briefly below and we empirically evaluate their performance over our dataset. The results are presented in Section IV.

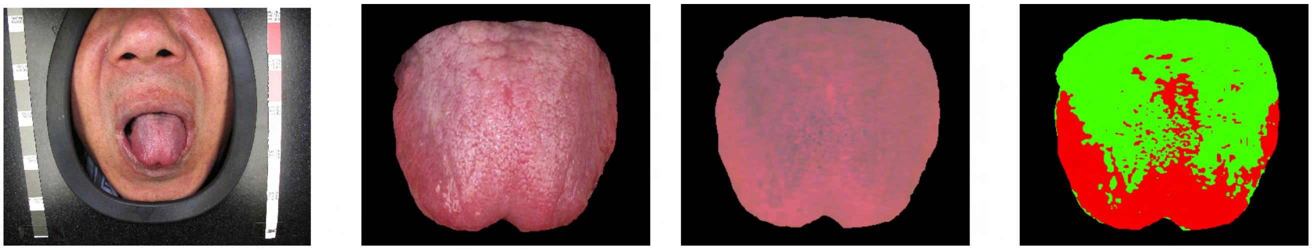

(a) Original Tongue Image (b) Segmented Image (c) MSF Image (d) Coating Separation Output

Figure 3. Illustration of the process of generating the coated region from a tongue image for use in feature extraction.

Table I
OVERVIEW OF THE COLOR FEATURES EXTRACTED.

Category	Brief Description	Feature Set
RGB	Additive color system based on trichromatic theory	$f_1^i = r_i, f_2^i = g_i, f_3^i = b_i.$
HSV	Represents color by 3-tuple set: hue, saturation and value	$f_4^i = h_i; f_5^i = s_i; f_6^i = v_i$
YIQ	Television transmission color space for a digital standard ([14] [15])	$f_7^i = y_i; f_8^i = i_i; f_9^i = q_i$
Y'CbCr	Television transmission color space for analogue NTSC system	$f_{10}^i = y_i'; f_{11}^i = cb_i; f_{12}^i = cr_i$
XYZ	Based on CIE XYZ color space ([16]) using brightness and chromaticity	$f_{13}^i = x_i; f_{14}^i = y"_i; f_{15}^i = z_i$
L*a*b*	Nonlinear transformation of CIE XYZ color space ([17])	$f_{16}^i = l_i^*; f_{17}^i = a_i; f_{18}^i = b_i$
L*u*v*	Derived from transformation of CIE XYZ color space for perceptual uniformity	$f_{19}^i = l_i^"; f_{20}^i = u_i; f_{21}^i = v_i$
CMYK	A subtractive color system ([16]) for the printing industry	$f_{22}^i = C_i; f_{23}^i = M_i; f_{24}^i = Y_i^*; f_{25}^i = K_i$

1) Support Vector Machine: The Support Vector Machine (SVM) [20] is one of the best-known general purpose learning algorithms. The goal of the SVM is to produce a model which predicts target values of data instances in the testing set given a vector of feature attributes. It attempts to maximize the margin of separation between the support vectors of each class and minimize the error in case the data is non-linearly separable. The SVM classifiers usually perform well in high-dimensional spaces, avoid over-fitting and have good generalization capabilities. For a given a training set $\{x_i, y_i\}_{i=1,..,n}$, the SVM model for an instance x can be written as [21]: The final hypothesis is given by

$$f(x) = \sum_{i=1}^{n} y_i \alpha_i k(x_i, x) + b \tag{9}$$

where k is the kernel function used (polynomial kernel in this work), α_i is the Lanrange multiple and b is a constant.

In our work, we utilize the Sequential Minimal Optimization (SMO) algorithm [22], which gives an efficient way of solving the dual problem of the support vector machine optimization problem.

2) Multilayer Perceptron Networks: The Multilayer Perceptron Network (MLP) [23] is a feed-forward neural network with one or more layers that are hidden from the input and output nodes. Neural networks have the ability to learn complex data structures and approximate any continuous mapping [24]. The model of each neuron in the network includes a nonlinear activation function that is differentiable such as the sigmoid. The units each perform a biased weighted sum of their inputs and pass this activation level through the transfer function to produce their output given by

$$\varphi(x) = f(w^T x + \theta) \tag{10}$$

where w is the synaptic vector, x is the input vector, θ is the bias constant, and T is the transpose operator. For K-class classification, the MLP uses back propagation to implement nonlinear discriminants. There are K outputs with softmax as the output nonlinearity.

3) Random Forest: A random forest [19] is a ensemble classifier consisting of a collection of tree-structured classifiers $\{h(\mathbf{x}, \Theta_k), k = 1, ...\}$ where the Θ_k are independent identically distributed random vectors and each tree casts a unit vote for the most popular class at input $\mathbf{x}$.

To apply the Random Forest method [25], initially draw n_{tree} from the original data. For each of the bootstrap samples, grow an unpruned classification tree. At each node, randomly sample m_{try} of the predictors and choose the best split from among those variables. Predict new data by aggregating the predictions of the n_{tree} trees using majority votes.

IV. Experimental Results and Analysis

The goal of the experiments presented in this section is to evaluate the performance of our modified ZHENG classification system using the 3 classification models to the original classification system proposed using the entire tongue to derive the features. Since we apply supervised learning methods, we rely on a labeled dataset to learn from. The dataset used consists of tongue images from 263 gastritis patients and a control group of 48 healthy volunteers. Most of the gastritis patients have been classified as Hot or Cold ZHENG and are identified with a color label (yellow or white) based on the observed color of the coating on their tongue, as determined by the TCM clinical practitioners. We are also interested in the relationship between TCM diagnosis and Western medicine diagnosis; hence, for a subset of the patients, we are provided with their corresponding Western medical gastritis pathology (superficial vs. atrophic). In Western medicine, the doctors are also interested in knowing whether the Helicobacter Pylori (HP) bacterium found in the stomach is present (positive) or absent (negative) in the patients with chronic gastritis. We have that information identified for a subset of the patients too. It was not feasible to obtain all the different information collected per patient. Table II summaries the population of each subset for four different labels (ZHENG, Coating, Pathology, and HP).

Table II
DATA LABEL SUMMARY FOR THE GASTRITIS PATIENTS.

Labels	Population
ZHENG: Hot/Cold	132 / 68
Coating: Yellow / White	147 / 67
Pathology: Superficial/Atrophic	84 / 144
HP bacterium: Positive / Negative	72 / 167

In training and testing our classification models, we employ a 4-fold cross-validation strategy. This implies that the data is split into three sets; one set is used for testing and the remaining three two sets is are used for training. The experiment is repeated with each of the three sets used for testing. The average accuracy of the tests over the four sets is taken as the performance measure. For each classification model, we varied the parameters to optimize its performance. We also compare the results obtained using the six different variations of the feature vector (Mean $=\mu\vec{F}$, Median $=med\vec{F}$, standard deviation$=\sigma\vec{F}$, mean + standard deviation= $\{\mu F, \sigma\vec{F}\}$, median + standard deviation $=\{medF, \sigma\vec{F}\}$), and mean + median + standard deviation= $\{\mu F, medF, \sigma\vec{F}\}$ as described in Section III-A. The results displayed highlight the best obtained from applying each of the six feature vectors.

The performance metrics used are the Classification Accuracy (CA) and the average F1 score (also known as F-measure). CA is defined as the percentage of correctly classified instances over the entire set of instances classified. The F1 score combines Precision (also known as True Positive Rate or Sensitivity) and Recall (or Positive Predictive Value (PPV)). It measures how well an algorithm can predict an instance belonging to a particular class. Let TP represent True Positive, which we define as the number of instances that are correctly classified as C_1 for a given test set while TN denotes True Negative, the equivalent for C_2 instances. Let FP represent False Positive, which we define as the number of instances that are incorrectly classified as C_1 for a given test set while FN denotes False Negative, the equivalent for C_2 instances. Precision $= TP/(TP+FP)$, and Recall $= TP/(TP+FN)$. Thus, the F1 score is defined as:

$$\text{F1-score} = \frac{2 \cdot \text{Recall} \cdot \text{Precision}}{\text{Recall} + \text{Precision}} \tag{11}$$

For both binary classes $\{C_1, C_2\}$, let $(|C_1|, |C_2|)$ denote the total number of instances belonging to class C_1 and C_2, respectively, then the average F1 score is defined as:

$$\text{F1-score}_{\text{avg}} = \frac{|C_1| \cdot \text{F1-score}(C_1) + |C_2| \cdot \text{F1-score}(C_2)}{|C_1| + |C_2|} \tag{12}$$

In Table III illustrating the different experimental results, we highlight the best F1-score$_{\text{avg}}$ (F1) obtained along with the corresponding Classification Accuracy (CA) of the classifier.

From the experimental results presented in Table III, we can draw the following conclusions. Firstly, applying the color features only to the coating region yielded better results in some cases but not all, compared to using the entire tongue image to extract the features. In making discrimination between the color of the coating on the tongue within the gastritis patients group, it is not sufficient only to restrict the feature extraction to the coated region. This is because we lose information by using only one component, the red channel, to extract the coated region from the tongue image. This also affects the performance of discrimination between Hot and Cold ZHENG patients. However, when we observe the performance of the classifiers with respect to the Western Medicine relations (presence of the HP bacterium and the pathology groups), using the coated region is more superior.

Secondly, when classifying the normal groups vs. the ZHENG groupings and the pathology groups, using the coated region outperformed our previous model generated with the entire tongue image. This is very interesting, as it strengthen the notion that using the MSF images to separate the coated region on the tongue prior to feature extraction is effective.

Thirdly, concerning the performance of the different classification models, we observe that the MLP and SVM models outperformed the Random Forest model. The RF model, like the Adaboost, is a simple model but not adequate to learn the complex relationships between the color features of the tongue images and the ZHENG/coating classes.

V. CONCLUSION

In this work, we proposed a coating separation technique using the MSF images such that feature extraction is applied only to the coated region on the tongue surface for TCM ZHENG classification. The results obtained demonstrate an improved performance for most of the classification types considered. We are able to more accurately discriminate between the Normal patients and the ZHENG groupings using our enhanced model. We also obtain a more superior

Table III
COMPARISON BETWEEN USING THE COATED REGION VS. ENTIRE TONGUE FOR CLASSIFICATION.

Classification Experiment Type	SVM		MLP		Random Forest		Entire Tongue	
	CA	F1	CA	F1	CA	F1	CA	F1
Coating (Yellow versus White)	0.802	0.789	0.778	0.775	0.764	0.745	**0.803**	**0.801**
ZHENG (Hot versus Cold)	0.700	0.701	0.740	0.738	0.735	0.721	**0.765**	**0.763**
HP Bacteria (Positive versus Negative)	0.732	0.734	**0.749**	**0.747**	0.724	0.692	0.720	0.713
Gastritis patients (Superficial versus Atrophic)	0.711	0.711	**0.728**	**0.724**	0.662	0.663	0.711	0.702
Hot ZHENG patients (Superficial versus Atrophic)	0.807	0.805	0.798	0.802	0.789	0.785	**0.844**	**0.845**
Cold ZHENG patients (Superficial versus Atrophic)	0.783	0.779	**0.817**	**0.815**	0.783	0.779	0.767	0.761
Superficial Patients (Hot versus Cold ZHENG)	0.838	0.838	**0.871**	**0.871**	0.855	0.853	0.839	0.839
Atrophic patients (Hot versus Cold ZHENG)	0.673	0.672	0.692	0.695	0.710	0.677	**0.738**	**0.734**
Normal group versus ZHENG patients	0.892	0.888	**0.911**	**0.908**	0.895	0.877	0.859	0.857
Normal group versus Hot ZHENG	**0.844**	**0.844**	0.839	0.838	0.806	0.793	0.822	0.828
Normal group versus Cold ZHENG	**0.819**	**0.820**	0.802	0.803	0.802	0.798	0.785	0.785
Normal group versus Superficial patients	**0.811**	**0.811**	0.795	0.797	0.788	0.783	**0.811**	**0.811**
Normal group versus Atrophic patients	0.792	0.793	**0.844**	**0.837**	0.813	0.796	0.839	0.837

performance for learning Western Medicine relationships among the gastritis patients. However, the performance is degraded in 2 main instances, when attempting to discriminate between the color on the coating on the tongue and also between Hot and Cold ZHENG patients. Our future work will be focused on modifications to make to the proposed system to further enhance its performance in this instances without degrading performance in other instances.

REFERENCES

[1] C. C. Chiu, H. S. Lin, and S. L. Lin, "A structural texture recognition approach for medical diagnosis through tongue," *Biomedical Engineering - Applications, Basis and Communications*, vol. 7, no. 2, pp. 143–148, 1995.

[2] C. C. Chiu, "The development of a computerized tongue diagnosis system," *Biomedical Engineering - Applications, Basis and Communications*, vol. 8, no. 4, pp. 342–350, 1996.

[3] C. Chiu, "A novel approach based on computerized image analysis for traditional chinese medical diagnosis of the tongue," *Computer methods and programs in biomedicine*, vol. 61, no. 2, pp. 77–89, 2000.

[4] C. H. Li and P. C. Yuen, "Tongue image matching using color content," *Pattern Recognition*, vol. 35, no. 2, pp. 407–419, Feb. 2002.

[5] B. Pang, D. Zhang, and K. Wang, "The bi-elliptical deformable contour and its application to automated tongue segmentation in chinese medicine," *IEEE Transactions on Medical Imaging*, vol. 24, no. 8, pp. 946–956, 2005.

[6] Z. Liu, J. Q. Yan, D. Zhang, and Q. L. Li, "Automated tongue segmentation in hyperspectral images for medicine," *Applied Optic*, vol. 46, no. 34, pp. 8328–8334, Nov. 2007.

[7] D. Zhang, Z. Liu, and J. Q. Yan, "Dynamic tongueprint: A novel biometric identifier," *Pattern Recognition*, vol. 43, no. 3, pp. 1071–1082, Mar. 2010.

[8] R. Kanawong, W. Xu, D. Xu, S. Li, T. Ma, and Y. Duan, "An automatic tongue detection and segmentation framework for computer-aided tongue image analysis," *International Journal of Functional Informatics and Personalized Medicine*, 2011.

[9] R. Kanawong, T. Obafemi-Ajayi, T. Ma, D. Xu, S. Li, and Y. Duan, "Automated tongue feature extraction for zheng classification in traditional chinese medicine," *Evidence-based complementary and alternative medicine : eCAM*, no. 912852, pp. 1741–427X, 2012.

[10] S. Li, Z. Q. Zhang, L. J. Wu, X. G. Zhang, Y. D. Li, and Y. Y. Wang, "Understanding zheng in traditional chinese medicine in the context of neuro-endocrine-immune network," *IET System Biology*, vol. 1, no. 1, pp. 51–60, 2007.

[11] H. Shen, H. Zhang, S. Shao, and J. H. Xin, "Chromaticity-based separation of reflection components in a single image," *Pattern Recognition*, vol. 41, no. 8, pp. 2461–2469, 2008.

[12] R. T. Tan, K. Nishino, and K. Ikeuchi, "Separating reflection components based on chromaticity and noise analysis," *Pattern Analysis and Machine Intelligence, IEEE Transactions on*, vol. 26, pp. 1373–1379, 2004.

[13] N. Otsu, "A threshold selection method from gray-level histograms," *IEEE Transactions on Systems, Man, and Cybernetic*, vol. 9, no. 1, pp. 62–66, 1979.

[14] Z. K. Huang and Z. F. Wang, "Bark classification using rbpnn in different color space," *Neural Information Processing*, vol. 11, no. 1, pp. 7–13, 2007.

[15] C. M. Tsai and Z. M. Yeh, "Contrast compensation by fuzzy classification and image illumination analysis for back-lit and front-lit color face images," *IEEE Transactions on Consumer Electronics*, vol. 56, no. 3, pp. 1570–1578, Aug. 2010.

[16] A. Ford and A. Roberts, "Colour space conversions," August 1998.

[17] M. Tkalcic and J. F. Tasic, "Colour spaces: perceptual, historical and applicational background," in *EUROCON 2003. Computer as a Tool. The IEEE Region 8*, vol. 1, Sept. 2003, pp. 304–308.

[18] Y. Freund and R. E. Schapire, "A decision theoretic generalization of on-line learning and an application to boosting," *Journal of Computer and System Sciences*, vol. 55, no. 1, pp. 119–139, 1997.

[19] L. Breiman, “Random forests,” *Machine Learning*, vol. 45, no. 1, pp. 5–32, 2001.

[20] C. J. Burges, “A tutorial on support vector machines for pattern recognition,” *Data Mining and Knowledge Discovery*, vol. 2, pp. 121–167, 1998.

[21] B. Scholkopf and A. Smole, *Learning with Kernals: Support Vector Machines, Regularization, Optimization, and Beyond.* The MIT Press, 2002.

[22] J. C. Platt, “Fast training of support vector machines using sequential minimal optimization,” in *Advances in Kernel Methods - Support Vector Learning*, 1998, p. 185.

[23] E. Alpaydin, *Introduction to Machine Learning*. MIT Press, 2004.

[24] A. Bouzerdoum, A. Havstad, and A. Beghdadi, “Image quality assessment using a neural network approach,” in *Proceedings of the Fourth IEEE International Symposium on Signal Processing and Information Technology*, 2004, pp. 330–333.

[25] A. Liaw and M. Wiener, “Classification and regression by random forest,” *R News*, vol. 2, no. 3, pp. 18–22, 2002.